which, in retrospect, provides an interesting structure for analysis of an immobilized complex.

The condition of excess ligand that prevented aggregation is pertinent for studies for which cupric ion or cupric-histidine complexes are present in complex biological media.[20] It is hypothesized that under certain conditions, that is in the presence of excess histidine, amino acid residues, upon freezing, may tend to form cupric complexes in which three or four nitrogen donor atoms are nitrogens from the imidazole ring and the amino nitrogen from histidine is released.

(20) Ettinger, M. J. In *Copper Proteins and Copper Enzymes*; Lontie, R., Ed.; CRC: Boca Raton, FL, 1984; Vol. III, p 181.

Registry No. L-his, 71-00-1; $Cu(his)_2$, 13870-80-9; ^{63}Cu, 14191-84-5; ^{15}N, 14390-96-6; D, 7782-39-0.

Contribution from the Gray Freshwater Biological Institute, University of Minnesota, Navarre, Minnesota 55392, and Department of Chemistry, State University of New York at Stony Brook, Stony Brook, New York 11794

Mössbauer and EPR Studies of a Synthetic Analogue for the Fe_4S_4 Core of Oxidized and Reduced High-Potential Iron Proteins

Vasilios Papaefthymiou,[†] Michelle M. Millar,[‡] and Eckard Münck*[†]

Received February 12, 1986

We have recently reported the synthesis and crystallographic characterization of the compound $(NBu_4)[Fe_4S_4(S\text{-}2,4,6\text{-}i\text{-}Pr_3C_6H_2)_4]$, a synthetic analogue for the $[Fe_4S_4]^{3+}$ cluster observed in oxidized high-potential iron proteins (HP). Here we report Mössbauer and EPR studies of this compound, both in polycrystalline form and in frozen solutions. Dissolved in toluene, acetonitrile, benzene, or dichloromethane, the synthetic complex displays EPR spectra very similar to those observed for oxidized HP, with $g_{av} \cong 2.06$. In polycrystalline form, however, the g values are smaller, with $g_{av} \cong 2.00$. In strong applied magnetic fields, well-resolved Mössbauer spectra are observed. The spectra are virtually identical in the polycrystalline state and in frozen toluene solution. We have analyzed the Mössbauer spectra in the framework of an $S = {}^1/_2$ spin Hamiltonian. As in HP the four iron sites occur in two equivalent pairs. For the two irons of each pair the hyperfine parameters are the same to within 5%. The set of hyperfine parameters match that of oxidized HP very well.

Introduction

More than a decade ago, it was established that the $[Fe_4S_4(S\text{-cys})_4]$ clusters of iron-sulfur proteins can exist in three different redox states, as represented by the following three-membered electron-transfer series:[1]

$$[Fe_4S_4]^{3+} \rightleftarrows [Fe_4S_4]^{2+} \rightleftarrows [Fe_4S_4]^{+}$$

$$[HP_{ox}] \rightleftarrows [HP_{red}, Fd_{ox}] \rightleftarrows [HP_{s\text{-}red}, Fd_{red}]$$

$$[Fe_4S_4(SR)_4]^{-} \rightleftarrows [Fe_4S_4(SR)_4]^{2-} \rightleftarrows [Fe_4S_4(SR)_4]^{3-}$$

In nature, the ferredoxins (Fd) utilize the $[Fe_4S_4]^{2+/+}$ core oxidation levels, while the so-called high-potential (HP) iron-sulfur proteins use the $[Fe_4S_4]^{3+/2+}$ core oxidation levels. Synthetic analogues were instrumental in the proof of the three-state hypothesis. In an extensive series of papers, Holm and his co-workers have described the synthesis and characterization of the $[Fe_4S_4(SR)_4]^{2-}$ and $[Fe_4S_4(SR)_4]^{3-}$ complexes.[2] Detailed structural and spectroscopic studies have demonstrated the congruence of these analogues with the biological $[Fe_4S_4]^{2+}$ and $[Fe_4S_4]^{+}$ clusters. We recently reported the synthesis and structural characterization of the first synthetic analogue containing the $[Fe_4S_4]^{3+}$ core.[3] That complex, $(NBu_4)[Fe_4S_4(SR_4)]$ with R = 2,4,6-*i*-$Pr_3C_6H_2$, corresponds to the oxidized form of high-potential iron-sulfur proteins (HP_{ox}).

The oxidized HP proteins have been studied by a wide range of physicochemical techniques, including Mössbauer,[4,5] EPR,[6,7] ENDOR,[8] NMR,[9] MCD,[10] and resonance Raman[11] spectroscopies as well as X-ray crystallography.[12] EPR spectroscopy has been useful in distinguishing the $[Fe_4S_4]^{3+}$ centers in HP_{ox} proteins from the EPR-active $[Fe_4S_4]^{+}$ centers of reduced ferredoxins and the $[Fe_2S_2]^{+}$ clusters of the Fe_2S_2 proteins. For several years, an EPR signal for iron-sulfur proteins with $g_{av} > 2$, which disappeared upon reduction, was assumed to be indicative of a $[Fe_4S_4]^{3+}$ center. This assumption was shown to be incorrect by the discovery that oxidized Fe_3S_n proteins and novel iron-sulfur centers in oxidized hydrogenase also display $g_{av} > 2$ EPR spectra. Mössbauer

Table I. g Values of $[Fe_4S_4]^{3+}$ Clusters in Proteins and Synthetic Complexes

	g_1	g_2	g_3	g_{av}	ref
R. gelatinosa HP	2.11	2.03	2.03	2.056	16
C. vinosum HP	2.12	2.04	2.04	2.07	6
	2.088	2.055	2.040	2.06	6
Ectothiorhodospira halophila HP	2.078	2.033	2.033	2.048	16
B center in irradiated $(NBu_4)[Fe_4S_4(SC_6H_5)_4]$	2.108	2.006	1.987	2.034	17
$(NBu_4)[Fe_4S_4(SR)_4]$ (benzene, dichloromethane, acetonitrile)	2.10	2.07	2.03	2.066	this work
$(NBu_4)[Fe_4S_4(SR)_4]$ (toluene)	2.10	2.05	2.03	2.060	this work
$(NBu_4)[Fe_4S_4(SR)_4]$ (polycrystalline)	2.065	1.97	1.96	2.000	this work

[†] University of Minnesota.
[‡] State University of New York at Stony Brook.

(1) Lovenberg, W., Ed. *Iron-Sulfur Proteins*; Academic: New York, 1973 (Vol. I and II), 1977 (Vol. III). Spiro, T. G., Ed. *Metal Ions in Biology*; Wiley-Interscience: New York, 1982; Vol. 4. Sweeney, W. V.; Rabinowitz, J. C. *Annu. Rev. Biochem.* **1980**, *49*, 139.
(2) Berg, J. M.; Holm, R. H. In *Metal Ions in Biology*; Spiro, T. G., Ed.; Wiley-Interscience: New York, 1982; Vol. 4, Chapter 1.
(3) O'Sullivan, T.; Millar, M. M. *J. Am. Chem. Soc.* **1985**, *107*, 4096.
(4) Dickson, D. P. E.; Johnson, C. E.; Cammack, R.; Evans, M. C. W.; Hall, D. O.; Rao, K. K. *Biochem. J.* **1974**, *139*, 105.
(5) Middleton, P.; Dickson, D. P. E.; Johnson, C. E.; Rush, J. D. *Eur. J. Biochem.* **1980**, *104*, 289.
(6) Antanaitis, B. C.; Moss, T. H. *Biochim. Biophys. Acta* **1975**, *405*, 262.
(7) Peisach, J.; Orme-Johnson, N. R.; Mims, W. B.; Orme-Johnson, W. H. *J. Biol. Chem.* **1977**, *252*, 5643.
(8) Anderson, R. E.; Anger, G.; Petersson, L.; Ehrenberg, A.; Cammack, R.; Hall, D. O.; Mullinger, R.; Rao, K. K. *Biochim. Biophys. Acta* **1975**, *376*, 63.
(9) Phillips, W. D.; Poe, M.; McDonald, C. C.; Bartsch, R. G. *Proc. Nat. Acad. Sci. U.S.A.* **1970**, *67*, 682. Nettesheim, D. G.; Meyer, T. E.; Feinberg, B. A.; Otvos, J. D. *J. Biol. Chem.* **1983**, *258*, 8235.
(10) Johnson, M. K.; Thomson, A. J.; Robinson, A. E.; Rao, K. K.; Hall, D. O. *Biochim. Biophys. Acta* **1981**, *667*, 433.

0020-1669/86/1325-3010$01.50/0

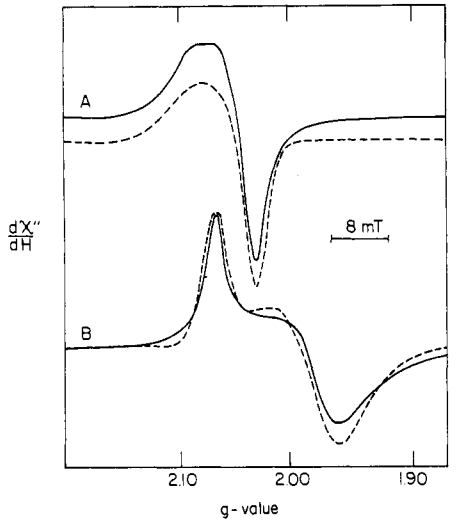

Figure 1. 9.23-GHz EPR spectra of $(NBu_4)[Fe_4S_4(SR)_4]$ in frozen toluene solution (A) and in the polycrystalline state (B). Dashed curves are spectra simulated for the parameters quoted in the text. Experimental conditions: (A) cluster concentration, 11 mM; T = 5 K; microwave power, 0.2 mW; modulation amplitude, 1 mT. (B) T = 9.2 K; 10 μW; 1 mT.

spectroscopy has been decisive in ruling out the occurrence of $[Fe_4S_4]^{3+}$ clusters in both of these cases.[13-15] In this paper, we report the Mössbauer and EPR spectra of the $[Fe_4S_4]^{3+}$ analogue and compare these spectra to those of the oxidized HP iron–sulfur proteins.

Materials and Methods

Crystalline $(NBu_4)[Fe_4S_4(SR)_4]$ was prepared as described previously.[3] Solution samples for Mössbauer and EPR studies were prepared by dissolving the polycrystalline material in degassed solutions of benzene, acetonitrile, toluene and dichloromethane under anaerobic conditions. EPR studies were carried out at X-band frequency by using a VarianE-109 spectrometer equipped with an Oxford ESR-10 liquid-helium cryostat. The Mössbauer spectra were obtained at 1.3–200 K by using Janis Research Super-Varitemp Dewars, one of them fitted with a superconducting magnet for studies in parallel fields up to 6.0 T. The Mössbauer source was ^{57}Co diffused into a rhodium matrix. All isomer shifts, δ, are quoted relative to Fe metal at 298 K.

EPR Studies. The $[Fe_4S_4]^{3+}$ cluster of oxidized HP has an electronic ground state with $S = {}^1/_2$. The protein from *Rhodopseudomonas gelatinosa*[16] for instance, exhibits g values at $g_1 = 2.11$ and $g_2 = g_3 = 2.03$, corresponding to $g_{av} = 2.056$. The protein from *Chromatium vinosum*, which has been thoroughly studied with X-ray diffraction and with a variety of physical techniques, exhibits two species with g values as listed in Table I.

The frozen-solution EPR spectra of $(NBu_4)[Fe_4S_4(SR)_4]$ depend very little on the solvent. A typical spectrum, obtained at 5 K in frozen toluene solution, is shown in Figure 1A (solid line). Also shown, for illustration of the qualitative features, is a spectral simulation (dashed curve) with $g_1 = 2.10$, $g_2 = 2.05$, and $g_3 = 2.03$, using Gaussian lines with 9, 8, and 3 mT along the three principal directions, respectively. As for oxidized HP, the spectrum has $g_{av} > 2$. In contrast to the sharp protein spectra ($\approx$1 mT width) the spectra of the synthetic complex have broad lines, reflecting considerable g strain.

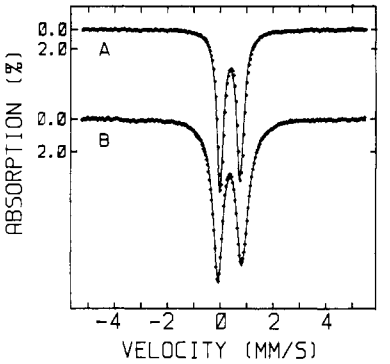

Figure 2. Zero-field Mössbauer spectra of the polycrystalline $[Fe_4S_4]^{3+}$ complex recorded at 100 (A) and 4.2 K (B). The solid line are least-squares fits for the parameters quoted in Tables II and III.

The EPR spectra of frozen acetonitrile, benzene, and dichloromethane solutions are essentially identical and are very similar to that shown in Figure 1A, except that the g values are slightly larger than those observed in toluene. In dichloromethane the power for half-saturation is $\approx$ 200 mW at 6 K; the spectrum was still detectable at 60 K.

The EPR spectrum of the polycrystalline material (solid line, Figure 1B) is quite distinct from those observed in frozen solution. The main features have shifted to lower g values. The dashed line is a theoretical spectrum computed with $g_1 = 2.065$, $g_2 = 1.97$, and $g_3 = 1.96$ with 4, 8 and 17 mT used for the widths. It is quite clear that the theoretical spectrum represents the experimental data quite poorly. This is, however, not surprising in view of the fact that we are dealing with a magnetically concentrated material containing Fe_4S_4 clusters that approach each other to 11.5 Å center–center. At this distance we can expect the spectrum to be affected by spin–spin relaxation, static dipolar, and exchange interactions. Since the dashed line of Figure 1B was obtained by assuming an isolated $S = {}^1/_2$ paramagnet, the quoted g values should be considered with some reservation.

Mössbauer Studies. Figure 2 shows zero-field spectra of a polycrystalline sample of $(NBu_4)[Fe_4S_4(SR)_4]$. The 150 K spectrum consists of a symmetric quadrupole doublet, characteristic of a paramagnetic complex with fast electronic spin relaxation. The 4.2 K spectrum displays a doublet as well, albeit with broadened lines. This observation in combination with the EPR signal of the polycrystalline material suggests that the electronic spin $S = {}^1/_2$ has intermediate ($k_1 \approx 10^8$–10^9 s^{-1}) relaxation rates at 4.2 K. Most likely, this relaxation results from intermolecular spin–spin interactions within the polycrystalline solid. We have studied the low-temperature spectra, $T \leq 4.2$ K, in applied fields up to 6.0 T, and we noticed that the spectra exhibit intermediate relaxation[18] as long as the "spin-up" state of the ground Kramers doublet is populated. Since the analysis of such spectra is immensely complex, we have chosen conditions where the "spin-up" state is not populated (T = 1.3 K, $H > 4.0$ T). Under these conditions the spectra of $S = {}^1/_2$ ($g \approx 2$) complexes do not depend on the relaxation rate.[19] Spectra recorded in 4.5 and 6.0 T applied parallel fields are shown in parts A and B of Figure 3, respectively.

The Mössbauer spectra obtained for *C. vinosum* HP samples have revealed that the four iron sites of the [4Fe-4S]$^{3+}$ core occur in two equivalent pairs.[5] Such equivalent pairs occur also for the synthetic complex studied here. We have therefore analyzed the spectra of Figure 3 with the $S = {}^1/_2$ spin Hamiltonian

$$\hat{H} = \beta\vec{S}\cdot\tilde{g}\cdot\vec{H} + \sum_{i=1}^{2}[\vec{S}\cdot\tilde{A}(i)\cdot\vec{I}(i) - g_n\beta\vec{H}\cdot\vec{I}(i) + \hat{H}_Q(i)] \quad (1)$$

$$\hat{H}_Q = \frac{eQV_{zz}}{12}[3I_z^2 - I(I+1) + \eta(I_x^2 - I_y^2)] \quad (2)$$

In eq 1 and 2 all symbols have their conventional meanings. We have described elsewhere the methodology of analyzing spectra as obtained here.[20] However, we would like to comment briefly on the spatial relationships between the parameters of eq 1. The **g** tensor of the synthetic complex is essentially isotropic. This implies that the Mössbauer

(11) Spiro, T. G.; Hare, J.; Yachandra, V.; Gerwith, A.; Johnson, M. K.; Remsen, E. In *Metal Ions in Biology*; Spiro, T. G., Ed.; Wiley-Interscience: New York, 1982; Vol. 4.
(12) Carter, C. W., Jr. In *Iron-Sulfur Proteins*; Academic: New York, 1977; Vol. III, pp 157–204.
(13) Münck, E. In *Metal Ions in Biology*; Spiro, T. G., Ed.; Wiley-Interscience: New York, 1982; Vol. 4.
(14) Wang, G.; Benecky, M. J.; Huynh, B. H.; Cline, J. F.; Adams, M. W. W.; Mortenson, L. E.; Hoffman, B. M.; Münck, E. *J. Biol. Chem.* **1984**, *259*, 14328.
(15) Huynh, B. H.; Czechowski, M. H.; Kruger, H.-J.; DerVartanian, D. V.; Peck, H. D., Jr.; LeGall, J. *Proc. Natl. Acad. Sci. U.S.A.* **1984**, *81*, 3728.
(16) Beinert, H.; Thomson, A. J. *Arch. Biochem. Biophys.* **1983**, *222*, 333.
(17) Gloux, J.; Gloux, P.; Lamotte, B.; Rius, G. *Phys. Rev. Lett.* **1985**, *54*, 599.

(18) Since the clusters approach each other to within 11.5 Å center–center, there may also be weak exchange interactions between adjacent clusters. According to our data, this interaction, if present, would be decoupled in an applied field of 6.0 T.

(19) Münck, E. *Methods Enzymol.* **1978**, *54*, 346.
(20) Christner, J. A.; Janick, P. A.; Siegel, L. M.; Münck, E. *J. Biol. Chem.* **1983**, *258*, 11157.

Table II. Hyperfine Parameters, at 4.2 K, of $(NBu_4)[Fe_4S_4(S\text{-}2,4,6\text{-}i\text{-}Pr_3C_6H_2)_4]$ in the $[Fe_4S_4]^{3+}$ Oxidized State[a]

	δ, mm/s	ΔE_Q, mm/s	η	A_x, MHz	A_y, MHz	A_z, MHz	A_{av}, MHz
				$(NBu_4)[Fe_4S_4(SR)_4]$			
α	0.40	−1.05	−4.0[b]	−28.8	−32.9	−34.3	−32.0
				(−28.1)	(−32.2)	(−32.9)	(−31.1)
β	0.34	−0.90	0.6	+22.6	+20.6	+17.4	+20.2
				(+21.9)	(+20.6)	(+18.5)	(+20.3)
				C. vinosum oxidized HP			
α	0.40	−1.03	0.9	−28.2	−30.6	−32.5	−30.4
β	0.29	−0.88	0.4	19.2	22.4	19.3	20.3

[a] The quoted set refers to the polycrystalline material. In parentheses the A values for the frozen toluene samples of Figure 3C are quoted; ΔE_Q, η, and δ are the same for the polycrystalline and solution samples. The uncertainties for the A values are estimated to be ±1 MHz. The isomer shifts, δ, are quoted relative to Fe metal at 298 K. Also listed are the parameters reported[5] for *C. vinosum* HP. The spatial coordinates in different rows are unrelated, i.e. x may refer to different orientations for each row. The A values of the synthetic complex can be aligned better with those of HP by a cyclic permutation. The reader may keep in mind, however, that the components of the EFG tensor need to be permuted in the same way since they are fixed relative to those of the A tensor. [b] One generally chooses a coordinate system for the EFG tensor such that $|V_{zz}| \geq |V_{yy}| \geq |V_{xx}|$. This choice restricts η to $0 \leq \eta \leq 1$. For a better comparison of the A values we have permuted the coordinates such that the components of the A tensor match those of HP best. A value of $\eta = -3$ corresponds to an EFG tensor that has axial symmetry around x.

spectra of polycrystalline samples do not convey information about the orientation of the magnetic hyperfine tensor A and the electric field gradient tensor [EFG tensor; principal components V_{xx}, V_{yy}, and V_{zz}; $\eta = (V_{xx} - V_{yy})/V_{zz}$; $\Delta E_Q = (eQV_{zz}/2)(1 + {}^1/_3\eta^2)^{1/2}$] relative to the g tensor. Since $\tilde{g}$ is the only quantity common to all Fe sites, the spatial orientations of the A and EFG tensors relative to the cluster are not determined. For each iron site, however, the relative orientations of the A and EFG tensors are determined. We have not obtained any evidence that the latter tensors have different principal axis systems.

The solid lines drawn through the data of parts A and B of Figure 3 are spectral simulations based on eq 1 and using the parameters listed in Table II. The following features have emerged from these simulations. (1) The spectra are well described by assuming that the four sites occur in pairs, labeled α and β. For each pair, the two sites are highly equivalent. From the sharpness of the two subspectra we can infer that the components of the A tensors of the two irons belonging to a pair cannot differ by more than about ±1 MHz. (2) The components of the magnetic hyperfine tensor of the α sites are negative whereas those of the β sites are positive. The signs are readily determined by observing whether the magnetic splittings of the subspectra increase ($A > 0$) or decrease ($A < 0$) as the strength of the applied field is increased. Since the local sites are tetrahedral and therefore high spin, the observation of positive A values implies that the local spins of the β sites are antiparallel to the system spin S. (3) The A tensors of both the α and β sites are quite isotropic. Within the uncertainties the α sites are axial. (See footnote *b* in Table II.) While the A tensor of the β sites is axial as well, the EFG tensor is rhombic. Finally, the α and β sites have different isomer shifts. The low-temperature data as well as the high-temperature data show that $\delta(\alpha) - \delta(\beta) \approx 0.06$ mm/s (Table III).

We have also studied the Mössbauer spectra of the oxidized complex dissolved in toluene. The zero-field spectra are essentially identical with those observed for the solid. At a cluster concentration of 11 mM, approximately 70% of the molecules exhibit paramagnetic hyperfine interactions at 4.2 K in an applied field of 60 mT, showing that the electronic spin of the majority of the molecules relax slowly; i.e., spin–spin interactions are reduced relative to the polycrystalline material. Although these low-field spectra were not as well resolved as those of Figure 3 their magnetic features are adequately described with the parameters of Table II. We have studied two such samples, with cluster concentrations of 11 and 22 mM, in a field of 6.0 T. The 6.0-T spectrum of the 22 mM sample (hashmarks) is shown in Figure 3C together with that obtained for the polycrystalline material (crosses). It can be seen that the splittings of the spectra of the β sites are virtually identical. (The β sites exhibit splittings in the 6.0-T spectra larger than those for the α sites because the external field is parallel to the internal field of the β sites and antiparallel to that of the α sites. Thus, the effective field is larger for the β sites.) The splittings for the α sites are slightly smaller in toluene solution. (There is a minor, perhaps 5% of total Fe, paramagnetic impurity present in the polycrystalline sample, as indicated by the shallow absorption around −3.5 mm/s and +4.5 mm/s in Figure 3A. The solution sample contains the impurity as well, at a slightly higher concentration. The presence of the impurity would allow us to normalize the spectra of Figure 3C differently and thus achieve a better agreement of the *intensities* of the outer absorption lines.)

For a comparison of the spectra of *C. vinosum* HP and our model compound we have plotted the theoretical spectra of HP in Figure 3D. The HP spectrum was computed with the parameters of Middleton et al.;[5] these parameters fit their experimental data very well.

Table III. Temperature Dependence of δ and ΔE_Q of the Polycrystalline Complexes Studied Here[a]

component	T, K	δ, mm/s	ΔE_Q, mm/s	Γ, mm/s
		$S = {}^1/_2$		
α	200	0.35	0.81	0.51
β		0.29	0.69	0.24
α	150	0.36	0.78	0.40
β		0.32	0.70	0.23
α	100	0.39	0.79	0.33
β		0.32	0.73	0.25
α	50	0.39	0.95	0.32
β		0.35	0.74	0.26
		$S = 0$		
	296	0.35	0.52	0.30
		0.35	0.52	0.30
	200	0.40	0.62	0.30
		0.40	0.62	0.30
	150	0.43	0.90	0.30
		0.43	0.67	0.30
	100	0.45	1.11	0.28
		0.45	0.85	0.28
	50	0.47	1.21	0.27
		0.46	1.02	0.27
	4.2	0.48	+1.25[b]	0.24
		0.47	+1.05	0.24

[a] All spectra were fitted with two symmetric doublets. For the $[Fe_4S_4]^{3+}$ complex the two sites are labeled corresponding to the components listed in Table II. Γ is the full width at half-maximum of the assumed Lorentzian lines. Isomer shifts are quoted relative to Fe metal at 298 K. The uncertainties for δ and ΔE_Q are estimated to be ±0.01 mm/s and ±0.02 mm/s, respectively. [b] The sign was determined from the fitting of the 6.0-T spectrum, $\eta \simeq 0.7$ (see eq 2), for both sites.

We have also studied the $[Fe_4S_4]^{2+}$ state, both in the solid and in a frozen solution. The 4.2 K Mössbauer spectrum of the polycrystalline material consists of a fairly sharp doublet (data not shown). Although the data are reasonably well represented by assuming one doublet, we obtained somewhat better fits by assuming two sites with slightly different quadrupole splittings. The parameters obtained and their temperature dependencies are listed in Table III. Spectra taken at 4.2 K in an applied field of 6.0 T show that the compound is diamagnetic ($S = 0$) and that both sites have $\Delta E_Q > 0$ and $\eta \cong 0.7$. Finally, we have studied the $[Fe_4S_4]^{2+}$ complex in toluene. The spectra were essentially the same except that the absorption lines were about 15% broader in toluene than in the solid.

Discussion

We have studied here the Mössbauer and EPR spectra of a model complex, containing the cubane Fe_4S_4 cluster, in both the 3+ and 2+ oxidation states. The low-temperature Mössbauer spectra of the oxidized complex exhibit beautifully resolved (Figure

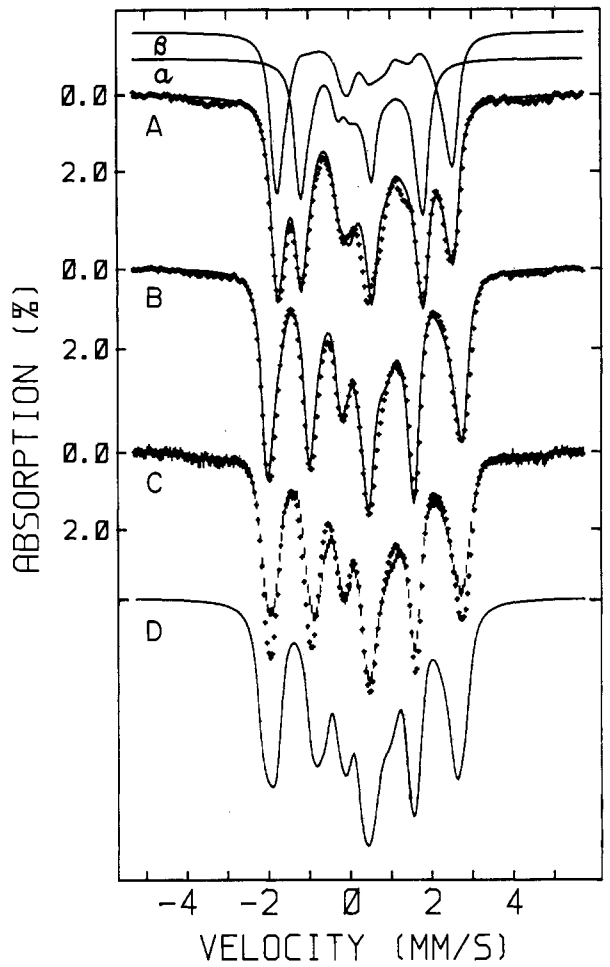

Figure 3. Mössbauer spectra of $(NBu_4)[Fe_4S_4(SR)_4]$ recorded at 1.3 K in parallel applied fields of 4.5 (A) and 6.0 T (B, C). The spectra in parts A and B were obtained on a polycrystalline sample whereas that (hashmarks) shown in part C was obtained with a 22 mM frozen toluene solution. Spectrum at 6.0 T is redrawn (crosses) in part C. The solid lines in parts A and B are spectral simulations using eq 1 with the parameters quoted in Table II. The subspectra of the α and β sites are separately drawn above the 4.5 T data. The curve in part D is a theoretical spectrum computed with the reported parameters of oxidized *C. vinosum* HP (see Table II).

3) magnetic hyperfine patterns. These spectra are much sharper than those reported for synthetic $[Fe_4S_4]^+$ clusters.[21,22] One interesting result of our studies is the observation that the four sites occur in two pairs, labeled α and β. We have concluded that the components of the magnetic hyperfine tensors of the two irons comprising each site are the same to within 5%; that is, if we allow any component of $\tilde{A}$ to differ by more than 5% for the two irons of each pair, we obtained fits that we judged to be noticeably inferior to those shown in parts A and B of Figure 3.

We found that the δ values for the α sites are about 0.06 mm/s more positive than those of the β sites. In terms of formal oxidation states, a precarious classification for these delocalized mixed-valence clusters, the α site comprises a Fe^{3+}–Fe^{2+} pair whereas the β site would consist of an Fe^{3+}–Fe^{3+} dimer. Note that the Fe^{3+}–Fe^{3+} pair has positive A values, suggesting that the projection of the local spins onto the $S = {}^1/_2$ system spin is negative. (A values of monomeric high-spin complexes are negative.) It is noteworthy that clusters with $[Fe_4S_4]^+$ core oxidation states exhibit pairs of equivalent iron sites as well.[20-25] It is of interest to know whether the odd electron in these clusters remains localized on one of the sites or whether electron hopping occurs among all four sites. For the *Desulfuribrio gigas* ferredoxin[24] and the cluster of aconitase[26,27] some information is available because one subsite in these clusters has been differentially labeled with ^{57}Fe by using $Fe_3S_4 \rightarrow Fe_4S_4$ cluster transformations. Mössbauer studies have shown that electron hopping does not occur over periods of months for $T < 150$ K.

Although much progress has been made recently toward an understanding of the electronic structure of iron–sulfur clusters[28] a good spin-coupling model for Fe_4S_4 clusters has not yet emerged. Suitable coupling models, using a Heisenberg Hamiltonian with isotropic exchange, have been put forward for Fe_2S_2 clusters[29] and two forms of oxidized Fe_3S_4 clusters.[30-32] A common feature of these clusters is the presence of localized valence states with properties reminiscent of rubredoxin-type monomers. Reduced Fe_3S_4[33] and Fe_4S_4 clusters, on the other hand, are delocalized mixed-valence systems for which an appropriate effective coupling Hamiltonian has not yet been developed. It has been pointed out[28,34,35] that electron delocalization gives rise to substantial resonance splitting in dimers and that, therefore, a Heisenberg Hamiltonian is not suitable for the description of such systems. Münck and Kent[33] have recently reviewed data on iron–sulfur clusters and have shown that the delocalized Fe^{3+}–Fe^{2+} pair of reduced *D. gigas* ferredoxin II has a dimer spin $S = {}^9/_2$. Formally, such a spin can arise from a parallel alignment of the spins of a high-spin Fe^{3+} ($S = {}^5/_2$) and Fe^{2+} ($S = 2$). Such an alignment can be the result of resonance interactions. A spin-coupling model for HP involving an Fe^{3+}–Fe^{3+} and an Fe^{3+}–Fe^{2+} pair has been discussed, in qualitative terms, by Middleton and co-workers.[5]

The $[Fe_4S_4]^{2+}$ core oxidation state is characterized by an isomer shift $\delta \approx 0.44$ mm/s, with a spread of about ± 0.03 mm/s, and quadrupole splittings ranging from about 0.8 to 1.5 mm/s at 4.2 K. Thus, δ is fairly constant whereas ΔE_Q shows considerable variability. Furthermore, ΔE_Q is independent of temperature in certain systems[36,37] while others exhibit a pronounced temperature-dependent ΔE_Q.[5,37] This variability in ΔE_Q and its temperature dependence reflects probably the disposition of the external ligands, in particular the orientation of the S–C bond. (That is, S–C_β–cys in proteins. However, the ligand structure in many proteins is unknown and non-sulfur ligands should also be considered.) In a theoretical study of the electronic structure of FeS_4 site of rubredoxin, Bair and Goddard[38] have pointed out that the

(21) Laskowski, E. J.; Reynolds, J. G.; Frankel, R. B.; Foner, S.; Papaefthymiou, G. C.; Holm, R. H. *J. Am. Chem. Soc.* **1979**, *101*, 6562. Laskowski, E. J.; Frankel, R. B.; Gillum, W. O.; Papaefthymiou, G. C.; Renaud, J.; Ibers, J. A.; Holm, R. H. *J. Am. Chem. Soc.* **1978**, *100*, 5322.
(22) Stephan, D. W.; Papaefthymiou, G. C.; Frankel, R. B.; Holm, R. H. *Inorg. Chem.* **1983**, *22*, 1550.
(23) Middleton, P.; Dickson, D. P. E.; Johnson, C. E.; Rush, J. D. *Eur. J. Biochem.* **1978**, *88*, 135.
(24) Moura, J. J. G.; Moura, I.; Kent, T. A.; Lipscomb, J. D.; Huynh, B. H.; LeGall, J.; Xavier, A. V.; Münck, E. *J. Biol. Chem.* **1982**, *257*, 6259.
(25) Lindahl, P. A.; Day, E. P.; Kent, T. A.; Orme-Johnson, W. H.; Münck, E. *J. Biol. Chem.* **1985**, *260*, 11160.
(26) Kent, T. A.; Merkle, H.; Emptage, M.; Kennedy, M. C.; Beinert, H.; Münck, E. *J. Biol. Chem.* **1985**, *260*, 6871.
(27) Kent, T. A.; Dreyer, J.-L.; Kennedy, M. C.; Huynh, B. H.; Emptage, M. H.; Beinert, H.; Münck, E. *Proc. Nat. Acad. Sci. U.S.A.* **1982**, *79*, 1096.
(28) Noodleman, L.; Baerends, E. J. *J. Am. Chem. Soc.* **1984**, *106*, 2316. Aizman, A.; Case, D. A. *J. Am. Chem. Soc.* **1982**, *104*, 3269. Noodleman, L.; Norman, J. G., Jr.; Osborne, J. H.; Aizman, A.; Case, D. A. *J. Am. Chem. Soc.* **1985**, *107*, 3418.
(29) Gibson, J. F.; Hall, D. O.; Thornley, J. H. M.; Whatley, F. R. *Proc. Natl. Acad. Sci. U.S.A.* **1966**, *56*, 987.
(30) Kent, T. A.; Huynh, B. H.; Münck, E. *Proc. Natl. Acad. Sci. U.S.A.* **1980**, *77*, 6574.
(31) Kennedy, M. C.; Kent, T. A.; Emptage, M.; Merkle, H.; Beinert, H.; Münck, E. *J. Biol. Chem.* **1984**, *259*, 14463.
(32) Girerd, J.-J.; Papaefthymiou, G. C.; Watson, A. D.; Gamp, E.; Hagen, K. S.; Edelstein, N.; Frankel, R. B.; Holm, R. H. *J. Am. Chem. Soc.* **1984**, *106*, 5941.
(33) Münck, E.; Kent, T. A. *Hyperfine Interact.* **1986**, *27*, 161.
(34) Belinskii, M. I.; Tsukerblat, B. S.; Gerbeleu, N. V. *Sov. Phys.—Solid State (Engl. Transl.* **1983**, *26*, 1142.
(35) Girerd, J.-J. *J. Chem. Phys.* **1983**, *79*, 1766.
(36) Christner, J. A.; Münck, E.; Janick, P. A.; Siegel, L. M. *J. Biol. Chem.* **1981**, *256*, 2098.
(37) Frankel, R. B.; Averill, B. A.; Holm, R. H. *J. Phys., Colloq.* **1974**, *35*, 107.

orientation of the S-C_β bond determines the spatial disposition of the sulfur lone pairs and thus influences the Fe-S bond. Similar conclusions have been drawn[28] from theoretical studies of Fe_2S_2 clusters. Noodleman and co-workers[28] have recently performed X_α calculations of an $[Fe_4S_4(SCH_3)_4]^{2-}$ complex and obtained for each site $\Delta E_Q = 1.08$, $\eta = 1.0$ and $\delta = 0.49$ mm/s, in excellent agreement with the results obtained here (Table III).

Acknowledgment. This work was supported by NSF Grant PCM 83-06964 and NIH Grant GM 32526.

Registry No. $(NBu_4)[Fe_4S_4(S\text{-}2,4,6\text{-}Pr_3C_6H_2)_4]$, 96455-61-7.

(38) Bair, R. A.; Goddard, W. A. *J. Am. Chem. Soc.* **1978**, *100*, 5669.

Contribution from the Thimann Laboratories, Department of Chemistry, University of California, Santa Cruz, California 95064, and Department of Chemistry, University of California, Berkeley, California 94720

Convenient Synthesis and Properties of $(R_4N)_2[Ni(SAr)_4]$ (Ar = C_6H_5, *p*-C_6H_4Cl, *p*-$C_6H_4CH_3$, and *m*-C_6H_4Cl) and the Structure of Tetraethylammonium Tetrakis(*p*-chlorobenzenethiolato)nickelate(II)

Steven G. Rosenfield, William H. Armstrong,† and Pradip K. Mascharak*

Received January 22, 1986

Reaction of $(Et_4N)_2NiCl_4$ and $(R_4N)(SAr)$ (Ar = C_6H_5, *p*-C_6H_4Cl, *m*-C_6H_4Cl, *p*-$C_6H_4CH_3$) in acetonitrile affords $(R_4N)_2[Ni(SAr)_4]$ in high yield. Syntheses of soluble nickel thiolates are not possible in protic solvents, where only insoluble polymeric materials are obtained. $(Et_4N)_2[Ni(S\text{-}p\text{-}C_6H_4Cl)_4]$ crystallizes in the monoclinic space group $P2_1/c$ with $a = 16.299$ (3) Å, $b = 15.464$ (3) Å, $c = 18.784$ (3) Å, $\beta = 109.17$ (1)°, and $Z = 4$. The structure, refined to $R = 3.5\%$, reveals a distorted tetrahedral arrangement of S atoms around Ni with the average Ni-S distance being 2.281 Å. Two S-Ni-S angles are ~90° while the average of the other four is close to 120°. Three of the four Ni-S vectors are coplanar with the corresponding phenyl rings. Unfavorable steric contacts between the ortho H atoms and Ni or S atoms do not allow either an idealized square-planar or a tetrahedral arrangement of thiolates around Ni. This together with the tendency of the Ni-S bonds to be coplanar with the phenyl rings gives rise to the observed distortion. The NMR spectra of $(R_4N)_2[Ni(SAr)_4]$ are assigned and discussed.

Recent EXAFS studies on active sites of hydrogenases[1] have estabilished sulfur ligation to nickel, and this finding has raised renewed interest in the chemistry of nickel thiolates. The discrete nickel-thiolato species with known structure include monomeric,[2] dimeric,[3a] linear[3b] and cyclic trimeric,[4] cyclic tetrameric,[5] cyclic hexameric,[6] and cyclic octameric[7] complexes. Since there is only one nickel atom present in the active sites of these enzymes, the structure and properties of monomeric nickel thiolates draw special attention. The only species reported in this category is $(Ph_4P)_2[Ni(SPh)_4]$;[2] $Ni(SR)_4^{2-}$ with R = alkyl have not been synthesized.[3b] The reported synthesis involves stepwise displacement of dithiosquarate (Dts^{2-}) ligands from $(Ph_4P)_2Ni(Dts)_2$ by PhS^- in hot acetonitrile. This procedure requires synthesis of dithiosquaric acid and the nickel complex $(Ph_4P)_2Ni(Dts)_2$. In our recent attempt to synthesize monomeric thiolato complexes of nickel from simple starting materials, we have discovered a straightforword, high-yield synthetic route to $[Ni(SAr)_4]^{2-}$ (Ar = C_6H_5, *p*-C_6H_4Cl, *p*-$C_6H_4CH_3$, *m*-C_6H_4Cl).[8] The structure of $(Et_4N)_2[Ni(S\text{-}p\text{-}C_6H_4Cl)_4]$ (**1**) has also been determined in order to reexamine the unusual distortions reported for $(Ph_4P)_2[Ni(SPh)_4]$.[2b,9] In addition to the synthetic and structural information, the NMR spectra and assignments of several arenethiolates of nickel are reported.

Experimental Section

Preparation of Compounds. The thiols were procured from Aldrich Chemical Co. $(Et_4N)_2NiCl_4$ was synthesized by following a standard procedure.[10] In the following preparations, degassed solvents were used and all manipulations were performed under an atmosphere of dry and pure dinitrogen.

Tetraalkylammonium Thiolates $(R_4N)(SR)$. Synthesis of $(Et_4N)(S\text{-}p\text{-}C_6H_4Cl)$ is a typical example. To a solution of 10 mmol of sodium methoxide (0.23 g sodium) in 60 mL of methanol were added an equivalent amount (1.45 g) of *p*-chlorobenzenethiol and, within 10 min, 2.1 g (10 mmol) of Et_4NBr. After the mixture was stirred for 1 h, the solvent was removed in vacuo. The oily residue was extracted with 80 mL of acetonitrile and the extract was filtered. The clear often pale yellow filtrate was used in the synthesis of the nickel complex.

$(Et_4N)_2[Ni(S\text{-}p\text{-}C_6H_4Cl)_4]$ (1). A 1.02-g (2.2-mmol) sample of $(Et_4N)_2NiCl_4$ was dissolved in 50 mL of acetonitrile, and this deep blue solution was slowly added with contant stirring to the tetraethylammonium *p*-chlorobenzenethiolate solution (10 mmol). The color rapidly turned dark red brown. After the addition was complete, the clear red brown mixture was stirred at room temperature for 1 h and then stored at -20 °C for 6 h. The dark crystals that separated during this period were filtered and recrystallized from 70 mL of warm (~40 °C) propionitrile. A 1.39-g (70%) yield of large blocks was collected by filtration, washed with 1:2 v/v acetonitrile/diethyl ether and dried in vacuo. Anal. Calcd for $C_{40}H_{56}N_2NiS_4Cl_4$: C, 53.74; H, 6.32; N, 3.13; Ni, 6.57; Cl, 15.88. Found: C, 53.83; H, 6.23; N, 3.10; Ni, 6.35; Cl, 15.86.

The mole ratios and amounts of reactants were the same in the following syntheses.

$(Et_4N)_2[Ni(SC_6H_5)_4]$. Tetraethylammonium benzenethiolate was extracted into propionitrile (40 mL). $(Et_4N)_2NiCl_4$ was dissolved in 40 mL of acetonitrile. Addition of nickel to the thiolate solution resulted in a deep red-brown mixture, which was filtered to remove a small amount

* To whom correspondence should be addressed at the University of California, Santa Cruz.
† University of California, Berkeley.

(1) Lindahl, P. A.; Kojima, N.; Hausinger, R. P.; Fox, J. A.; Teo, B.-K.; Walsh, C. T.; Orme-Johnson, W. H. *J. Am. Chem. Soc.* **1984**, *106*, 3062. Scott, R. A.; Wallin, S. A.; Czechowski, M.; DerVartanian, D. V.; LeGall, J.; Peck, H. D., Jr.; Moura, I. *J. Am. Chem. Soc.* **1984**, *106*, 6864.
(2) (a) Holah, D. G.; Coucouvanis, D. *J. Am. Chem. Soc.* **1975**, *97*, 6917. (b) Swenson, D.; Baenziger, N. C.; Coucouvanis, D. *J. Am. Chem. Soc.* **1978**, *100*, 1932.
(3) (a) Lane, R. W.; Ibers, J. A.; Frankel, R. B.; Papaefthymiou, G. C.; Holm, R. H. *J. Am. Chem. Soc.* **1977**, *99*, 84. (b) Watson, A. D.; Rao, C. P.; Dorfman, J. R.; Holm, R. H. *Inorg. Chem.* **1985**, *24*, 2820.
(4) Tremel, W.; Krebs, B.; Henkel, G. *Inorg. Chim. Acta* **1983**, *80*, L31. Henkel, G.; Tremel, W.; Krebs, B. *Angew. Chem., Int. Ed. Engl.* **1983**, *22*, 319
(5) Gaete, W.; Ros, J.; Solans, X.; Font-Altaba, M.; Briansó, J. L. *Inorg. Chem.* **1984**, *23*, 39.
(6) Woodward, P.; Dahl, L. F.; Abel, E. W.; Crosse, B. C. *J. Am. Chem. Soc.* **1965**, *87*, 5251.
(7) Dance, I. G.; Scudder, M. L.; Secomb, R. *Inorg. Chem.* **1985**, *24*, 1201.
(8) As the manuscript for this paper approached completion, a brief report on a similar preparative route to $(Et_4N)_2[Ni(SPh)_4]$ appeared: Yamamaura, T.; Miyamae, H.; Katayama, Y.; Sasaki, Y. *Chem. Lett.* 1985, 269.
(9) Coucouvanis, D.; Swenson, D.; Baenziger, N. C.; Murphy, C.; Holah, D. G.; Sfarnas, N.; Simopoulos, A.; Kostikas, A. *J. Am. Chem. Soc.* **1981**, *103*, 3350.
(10) Gill, N. S.; Taylor, F. B. *Inorg. Synth.* **1967**, *9*, 136.

0020-1669/86/1325-3014$01.50/0